Swelling of Zwitterionic Polymer Films Characterized by Spectroscopic Ellipsometry

Y. Tang and J. R. Lu*

Department of Physics, UMIST, P.O. Box 88, Sackville St. Manchester M60 1QD, UK

A. L. Lewis, T. A. Vick, and P. W. Stratford

Biocompatibles Ltd., Farnham Business Park, Farnham, Surrey GU9 8QL, UK

Received March 19, 2001; Revised Manuscript Received August 21, 2001

ABSTRACT: The swelling of thin biocompatible polymeric films under water has been characterized by spectroscopic ellipsometry. The films were formed by coating a copolymer (PC 100B) onto optically flat silicon oxide surface. PC 100B has a polymethacrylate backbone bearing pendent zwitterionic phosphorylcholine (PC) groups (23 mol %), lauryl chains (47%), 2-hydroxypropyl groups (25%), and trimethoxysilane groups as cross-linker (5%). Film swelling as a result of water sorption was monitored by following the change in two ellipsometric angles (ψ and Δ) with time using dry films of a wide range of thickness. The swelling pattern was characterised by two distinct stages, an initial diffusion-controlled fast swelling, followed by a subsequent slower process controlled by the relaxation of polymer fragments. Although the fast initial stage occurred within the first minute of film immersion in water, some 50% water was absorbed into the films during this period. The rate of swelling in the second stage showed a steady decrease with the increasing annealing temperature. The equilibrated water content ($f_{w,\infty}$) was found to be some 60% for films annealed at 50 °C, 45% at 100 °C, and 30% at 150 °C, thus indicating that as the silyl network is strengthened with temperature its capacity for water uptake is suppressed. The values of $f_{w,\infty}$ calculated from the refractive indices of the films were broadly consistent with those determined separately from the increase in film thickness. This observation suggests that the swelling is almost linear over the period of the experiment and scales with the initial sample volume. The result is consistent with the assumption of homogeneous swelling used in the modeling and rules out any case II type of water distribution within these PC hydrogel films.

Introduction

When a solid polymer is in contact with a penetrant solvent, the polymer usually swells as the penetrant diffuses into it. The process of diffusion involves the transportation of the penetrant molecules into the existent voids or the spaces created between the polymer chains during the dynamic movement. Thus, swelling forces segmental motion within the polymer, resulting in the increased distance between polymer segments. This segmental expansion is often transformed into a macroscopic increase of the diameter for polymer particles or of the thickness for flat polymer films.

The transport of water and organic solvents (e.g., methanol, acetone, and hexane) into model polymers such as poly(methyl methacrylate) (PMMA) and poly(styrene) (PS) has been extensively studied in the literature.[1−8] These studies often use polymeric particles or polymer films of the dimensions of the order of millimeters so that the basic conditions for Fickian sorption, e.g., the constant concentrations at the two boundaries and a steady transport of penetrant, are satisfied.[9] In contrast, we have recently described a family of phosphorylcholine-based biocompatible polymer films that are used in biomedical applications, in which the film thicknesses are usually below a few micrometers. In addition, these biocompatible polymers often contain chemical components with a wide range of hydrophobicities. The coexistence of hydrophilic and hydrophobic fragments may promote the formation of structured morphology within the film that may deter the process of water transport. These limitations imposed by practical applications may mean that the swelling of biocompatible polymer films may not follow the classical Fickian diffusion process.

As one of the most important drug delivery mechanisms, the swelling of polymer hydrogels in aqueous environment has recently been paid much attention in the field of controlled drug delivery.[10,11] For a given polymeric hydrogel, the pattern of its swelling reflects the dynamic process of water penetration and hence the encounter of the incorporated drug with water. Thus, by altering the swelling of the polymeric carrier, the pattern of drug release may be adjusted. The PC polymer to be studied in this work (PC 100B) is an acrylic copolymer containing hydrophobic dodecyl chains and two types of hydrophilic component: phosphorylcholine groups (PC) and 2-hydroxypropyl groups. In addition, a few percent of silyl cross-linking groups are also incorporated into the copolymer. When the coated films are subject to annealing, the silane groups cross-link with themselves, the organic hydroxyl groups within the film or the hydroxy groups on the surface of solid substrate, resulting in the mechanical stability of the film. As already indicated above, the energetically unfavorable alignment between hydrophobic and hydrophilic moieties may promote segregation within the film, leading to the formation of lamellar layering or other types of aggregation. These microscopic morphologies within the polymeric film will constrain the exposure of certain polymeric fragments and slow down their swelling. For films coated at the room tempera-

* To whom correspondence should be addressed. E-mail j.lu@umist.ac.uk; Tel 44-161-2003926.

10.1021/ma010476i CCC: $20.00
Published on Web 11/03/2001

ture, segregation is unlikely to occur. However, annealing will help to release the stress within the films and will promote the segregation between fragments to minimize the total free energy. At the same time, increase in annealing temperature will intensify silyl cross-linking, and the strengthened silyl network will exert further resistance to the film expansion. It is useful to examine how the two combined processes affect dynamic process of film expansion and the equilibrated water content within the films.

In most of the existent literature studies, the dynamic process of solvent sorption is largely monitored by following the change of the weight of polymer films or particles with time,[9,12] and information about the molecular events has to be inferred from these data. Although these gravimetric measurements provide reasonable estimates of the overall amount of penetrant sorbed into the polymer matrix, no information is gained about the distribution of the solvent across the polymer and the variation of the structure of the film with time. Techniques such as ion beam analysis, FTIR-ATR,[13] magnetic resonance imaging,[14] and STRAFI[15−17] are the established methods for concentration profiling, but the range of film thickness that is of interest to biomedical coatings as already outlined above falls in the margin of instrumental resolution for some of these techniques. A number of recent studies have shown that surface plasmon resonance (SPR),[18,19] interferometry,[20,21] neutron reflectivity (NR),[22−24] and spectroscopic ellipsometry (SE)[25,26,27] are appropriate for studying thin polymer films with thicknesses typically less than 1 μm and under aqueous environment. These techniques also allow us to detect the possible uneven distributions of penetrants across the thin films.

Ellipsometry is an established technique for monitoring the dynamic and equilibrium properties at different interfaces.[26−28] In comparison with the conventional ellipsometers using single wavelength laser sources, variable angle spectroscopic ellipsometry offers flexibility for performing measurements over a range of wavelengths at different angles of incidence. Since the thickness of the films studied in this work ranged between a few hundred angstroms and 1 μm and was comparable to the wavelength range of the light source, ellipsometry was ideally suited for the characterization of these polymer films.

The investigation of the dynamic and equilibrium properties of PC 100B films is part of our continuing interests in the characterization of this type of hydrogels. In a previous work the surface biocompatibility of this polymer has been studied.[29−31] Films coated over a wide range of thicknesses and under various coating conditions were found to be highly effective at inhibiting nonspecific adsorption of blood proteins. Furthermore, it was found that the high surface biocompatibility of the polymer did not show sensitive variation with chemical composition of the polymer, thus making it versatile to a wide range of applications. The characterization of its swelling process constitutes a major step in our effort to understand this type of zwitterionic polymeric biomaterial. Furthermore, because the chemical structure of PC 100B resembles several polymeric hydrogels currently used in biomedical coatings,[32,33] this work will consolidate the relationship between the molecular structure of the polymers and their performance.

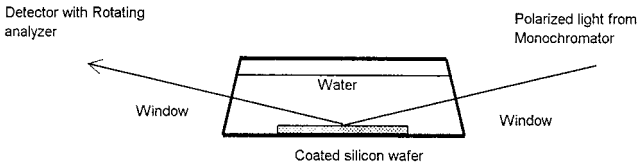

Figure 1. Schematics of sample cell with coated silicon wafer underneath.

Experimental Section

Materials. PC 100B (also known as PC 1036) was synthesized by copolymerizing lauryl methacrylate (LM, 47 mol % from Aldrich), methacryloyloxyethylphosphorylcholine (MPC, 23% Biocompatibles Ltd.), 2-hydroxypropyl methacrylate (HPM, 25% from Aldrich), and trimethoxysilylpropyl methacrylate (TPM, 5% from Aldrich), and the detailed synthetic procedure was described in refs 32 and 33. The polymerization was initialized using 1% AIBN (α,α'-azoisobutyronitrile), and the reaction was carried out at 62 °C in ethanol. The polymer was purified by double precipitation into acetone, typically yielding between 70 and 90% of a free white powder which was stored at −18 °C until required. Silicon wafers were purchased from Compart Technology Ltd. and were cleaned by immersing the wafers in dilute basic Decon solution (5%), followed by rinsing with Elgastat ultrapure (UHQ) water. Hexane and absolute ethanol from Aldrich (AR grades) were used as received.

Film Preparation. Thin PC polymer films were prepared by dip-coating silicon wafers in PC polymer solutions using a specifically designed coating rig as described in ref 31. The mixture of hexane and ethanol in the volume ratio of 1:1 was used as solvent. For preparing films with thickness between 500 and 8000 Å, polymer solutions at different concentrations were made. To remove possible insoluble particles, the solutions were filtered through paper filters with pore diameters around 1 μm. Varying solution concentrations together with different motor lifting speeds helped to produce films with required thickness and consistent uniformity. The coated films were dried in air for at least 2 h at room temperature before they were annealed at 50, 100, or 150 °C for 3 h under vacuum. The samples were then left to cool to room temperature naturally and were then kept in a vacuum desiccator for subsequent characterization.

Ellipsometry. The thickness and optical constants of polymer films coated on silicon oxide substrate were measured with a variable angle spectroscopic ellipsometry (VASE, J.A. Woollam Co.). The sample cell utilized is schematically shown in Figure 1. The temperature inside the cell was controlled by two circulating water bath attached on the wall of the cell. The coated wafer was positioned in the central area of the cell and was held by a sample holder (not shown). The beam was directed to the sample surface at an incidence angle of 74.5 °C with respect to the surface normal. The sample cell has two fixed windows on the incoming and exiting sides, and both windows were aligned perpendicular to the beams. The ellipsometric measurement was usually started with alignment at the air/solid interface first, followed by the determination of the thickness and refractive indices of the dry film in open air. Water was then introduced into the sample cell, and the subsequent autoscans were repeated at the solid/solution interface. The two ellipsometric angles ψ and Δ were recorded simultaneously over typical wavelengths between 350 and 700 nm. The time required for each scan over this wavelength range was determined by the rotation frequency of the analyzer and the number of pairs of ψ and Δ counted. It typically took some 40 s to complete a scan involving some 30 pairs of ψ and Δ at a rotational frequency of 30 s^{-1}.

The ellipsometric data were analyzed to obtain the best-fit film thicknesses and refractive indices using a Levenberg−Marquardt algorithm.[34] In the data fitting process, we assumed a uniform density distribution for the polymer chains and hence a uniform density profile for the water across the film.

Because the films were overall very thin, the water may diffuse from the outer film surface to its inner surface within seconds. This time scale is in contrast to about a minute required to complete the first spectroscopic scan. The spectroscopic measurements will thus have limited sensitivity to the initial swelling process.

For simplicity, we assume that water diffusing and film swelling occur in the direction perpendicular to the plane of the film. Meanwhile, we also assume that the area of the in-plane polymer in contact with water is much greater than in the edge so that the edge effect of the film could be ignored.[9] The instantaneous volume fraction of water, f_w, within the film at time t is

$$f_w = \frac{V_t - V_0}{V_t} = \frac{\tau - \tau_0}{\tau} \quad (1)$$

where V_t and τ are the swollen film volume and film thickness at time t, and V_0 and τ_0 are the dry film volume and film thickness, respectively. Following this linear relationship, the fraction of water uptake within the thin polymer film with respect to the final equilibrated amount can be calculated using the following equation:

$$\frac{M_t}{M_\infty} = \frac{f_w V_t}{f_{w,\infty} V_\infty} = \frac{\tau - \tau_0}{\tau_\infty - \tau_0} \quad (2)$$

where $V_t = A\tau$ and $V_\infty = A\tau_\infty$ (A is the surface area of the polymer film in contact with water and is assumed not to change with film swelling), M_t is the mass of water absorbed at any time t, M_∞ is the water amount at equilibrium, $f_{w,\infty}$ is the volume fraction of water at equilibrium, V_∞ is the equilibrium volume of the swollen polymer film, and τ_∞ is the equilibrium thickness of the polymer film.

A useful check of instrumental consistency is to compare the thickness at the air/solid with that for the same film determined at the solid/water interfaces. This process helps to ensure that the contribution of water as a medium at the solid/water interface is taken into account appropriately and the equipment is correctly characterized. In addition, since the main swelling occurs within the first 20 min of water addition as will be seen later, it is important to ensure that the instrumental signal is stable within this time scale and beyond. Obviously, the consistency of instrumental performance cannot be examined using films that swell under water, and hence PC 100B itself is unsuitable. Because polystyrene (PS) does not swell under water, PS films coated on silicon were used for this purpose. Figure 2 compares the plots of ψ and Δ measured at the solid/water interface after some 20 min of film immersion in water with those calculated from the dry film thickness of 1850 Å obtained at the air/solid interface before water was added. The calculation assumed that apart from taking water as medium (instead of air) other parameters were kept the same as those at the air/solid interface. The good agreement between the two sets of data suggests no measurable swelling of the film as expected, hence a good instrumental consistency and stability. It should be added that the scans of ψ and Δ profiles within the first minute of immersion of the PS film in water were also recorded, and the data overlapped well with those shown in Figure 2. The PS film was coated using the same coating procedure as described above and was annealed in a vacuum oven at 160 °C overnight.

The thickness of the dry PS film was obtained by fitting a single uniform layer to the ellipsometric profiles measured at the interface, and the best fit produced a value of 1850 ± 50 Å (shown as continuous lines in Figure 2). In fitting the uniform layer model, the dispersion of the refractive index was described analytically as

$$n(\lambda) = n_0 + \frac{C_1}{\lambda^2} + \frac{C_2}{\lambda^4} \quad (3)$$

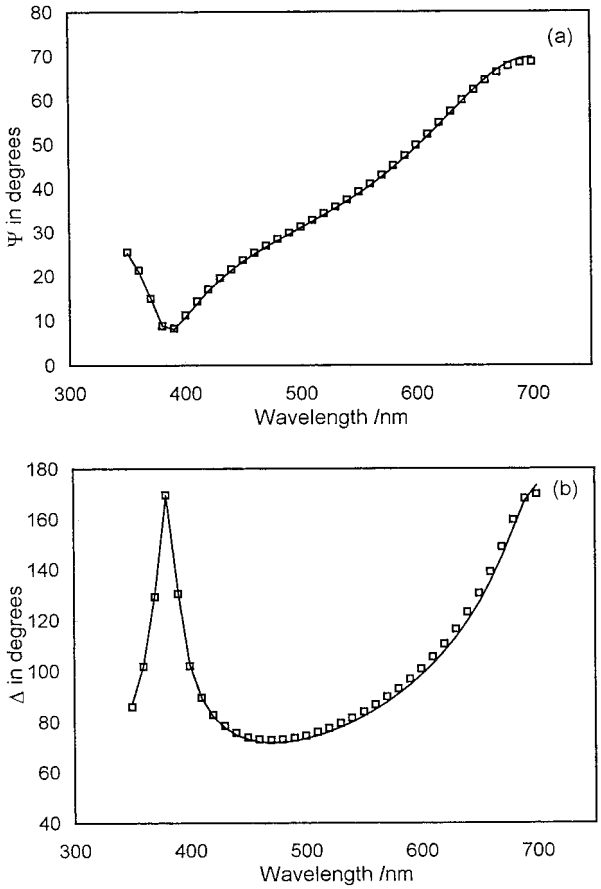

Figure 2. Ellipsometric angles of ψ (a) and Δ (b) scans against wavelength measured at the solid/water interface for a polystyrene film coated on silicon oxide wafer after 20 min of immersion in water. The dry polystyrene film was 1850 ± 50 Å thick and was dip-coated and subsequently annealed at 160 °C. The continuous lines were calculated by taking the thickness and refractive index of the PS film the same as the dry one. The good agreement between the calculated and measured data suggests no swelling of the film and a good instrumental reliability.

where λ is the wavelength of the beam, and n_0, C_1, and C_2 are the constants obtained from data fitting.[27,34,35] From the fitting of PS data, the refractive indices for the film were found to be the same as the bulk PS polymer, and apart from the account of the difference between air and water as the two bulk media and minor allowance to take the effect of windows into account, no other adjustments had to be made. This observation confirmed the absence of water inside the film. It should be noted here that for film thickness under a few hundred angstroms τ and n are interrelated, and it may be difficult to decouple τ and n from the ellipsometric data fitting.[35]

Results and Discussion

Using the experimental procedure established from the PS film measurement, we first examined the swelling of a thin PC 100B film annealed at 50 °C at the solid/water interface, and the resultant pairs of ψ and Δ are shown in Figure 3. Prior to the addition of water to the sample cell, measurement at the air/solid interface was made. Data fitting produced a dry film thickness of 610 ± 20 Å. This thickness together with the dry film refractive index enabled us to calculate the equivalent ψ and Δ profiles against λ at the solid/water interface at $t = 0$. This was the hypothetical point at which the bulk water was added but no swelling had occurred. This set of ψ and Δ profiles (shown as dashed lines in Figure 3) served as references for assessing the subse-

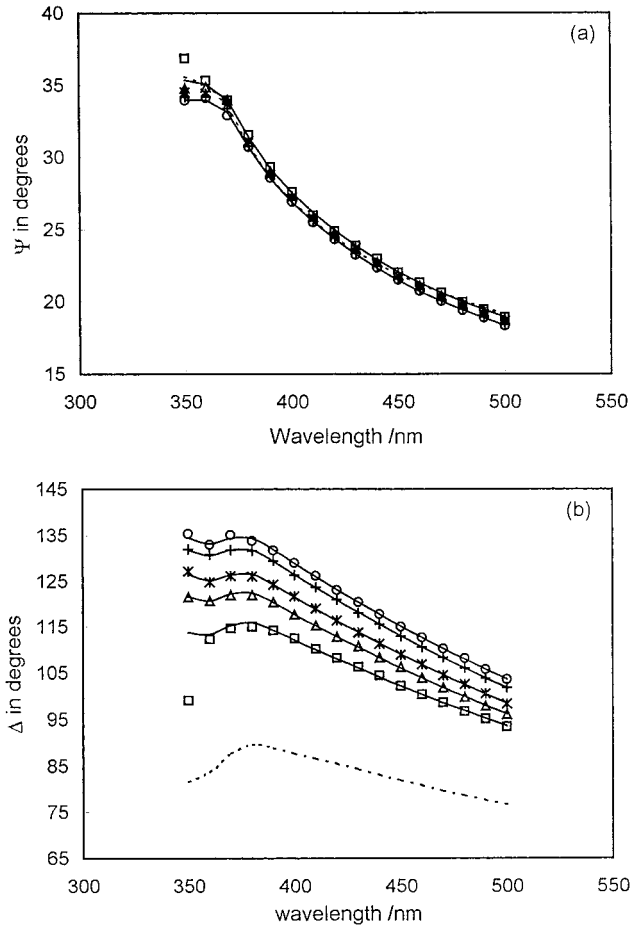

Figure 3. Variation of ψ (a) and Δ (b) with time for the swelling of a thin PC100B film with a dry film thickness of 610 ± 20 Å and annealed at 50 °C. The continuous lines are the best fits with structural parameters shown in Figure 4. The dotted lines were calculated assuming the film was immersed without any swelling or water penetration. The symbols represent the measurements at 1 (□), 3 (△), 6 (*), 16 (+), and 27 min (○) after water immersion.

quent swelling. As shown in Figure 3, the large gap between the calculated pair and the first set of the measured profiles (shown more clearly in □ in Figure 3b) indicates that a significant extent of swelling had already occurred within the first minute of film immersion in water. The subsequent changes in ψ and Δ are less dramatic, showing that after the first minute of contact with water the rate of swelling has slowed down. Figure 3 shows that while relatively small changes occur between ψ, much greater shifts are seen between Δ. As will be seen later, such relative progression in ψ and Δ is more strongly dictated by the dry film thickness. It should also be noted that since each scan took about 40 s, the first pair of ψ and Δ profiles represented the average of the changes within this period after film immersion in water. As the time evolved, the fraction of the time required for data collection became less significant, and the scans were closer to snapshots.

The measured ellipsometric profiles were analyzed using the single uniform layer fits as outlined previously. The continuous lines shown in Figure 3 are the best fits with the resultant τ and n shown in Figure 4. The volume fraction of water (f_w) within the film at a given time t can be calculated from the Lorentz−Lorenz equation using an effective medium approximation[36]

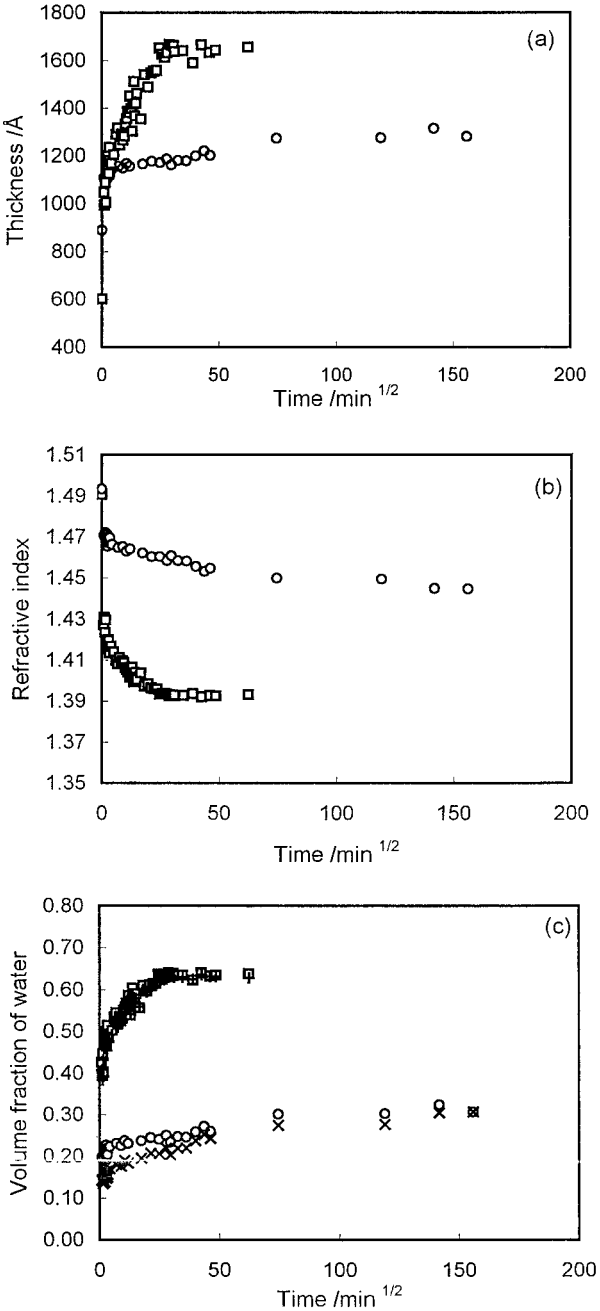

Figure 4. Change of thickness (a), refractive index (b), and water volume fraction (c) with time for the thin PC 100B films annealed at 50 (□) and 150 °C (○). Also in (c), the water volume fraction calculated from the change of thickness during film swelling is shown as (+) from the film annealed at 50 °C and as (×) from the film annealed at 150 °C.

$$f_w = \left[\frac{n^2 - n_p^2}{n^2 + 2n_p^2}\right] \Big/ \left[\frac{n_w^2 - n_p^2}{n_w^2 + 2n_p^2}\right] \qquad (4)$$

where n_w is the refractive index of water ($n_w = 1.333$ at $\lambda = 500$ nm) and n_p is the refractive index of the polymer at the same wavelength ($n_p = 1.480$ at $\lambda = 500$ nm). Alternatively, f_w can be obtained from ellipsometric thickness according to eq 1. The consistency in f_w between the two methods will offer some justification about the reliability in separating τ from n from the model fitting.

Because in conventional sorption studies the extent of swelling in terms of weight gain is usually plotted

against $t^{0.5}$ to reflect the main feature of the Fickian sorption kinetics,[9] the same approach has been adopted in this work. It can be seen from Figure 4 that for the dry film of 610 Å annealed at 50 °C the main increase in thickness occurs within the first few minutes of its immersion in water. Within this region, the thickness is almost linearly going up with $t^{0.5}$, indicating a characteristic feature of Fickian sorption at this stage. The large expansion of the film thickness is concurrent with the decline of refractive index, and the exact volume fraction of water within the layer was calculated from eq 4, with the resultant f_w shown in Figure 4c. As can be seen from Figure 4c, some 50% water was incorporated into the film within the first 10 min of immersion. This corresponds well to the extent of film thickness expansion. Saturation of the film was reached after some 20 h, and the final water volume fraction ($f_{w,\infty}$) is around 60%.

Similar measurement was made for the film with its dry thickness at 850 Å, but annealed at 150 °C. The results are also shown in Figure 4 for comparison. Again, there is a sharp initial increment of film thickness, accompanied by a fast water uptake, though the magnitude of film expansion and extent of water uptake within this initial period are much less than the film annealed at 50 °C. After this initial period, it took much longer for the swelling to reach equilibration. The final equilibrated water fraction is just about 30%, as compared with some 60% observed for the film annealed at 50 °C. This observation clearly shows the strong effect of annealing temperature on the degree of film swelling (expansibility) and the equilibrated water content within the films.

As already indicated previously, f_w can also be calculated from the increment in film thickness using eq 1. Because τ and n were decoupled from the model fitting, the determination of f_w from τ offers an alternative route for checking the self-consistency of the data. The comparison is shown in Figure 4c. Both sets of f_w are in a good agreement for the film annealed at 50 °C, though the agreement is less good for the films annealed at 150 °C. The largest difference in f_w is about 10%, and the extent of deviation indicates the degree of interrelation between τ and n for such thin films. We have indicated previously that when film thickness is very ultrathin, less than a few hundred angstroms, it becomes difficult to decouple τ and n based on the data fitting alone.[37]

To substantiate these findings and to reduce the extent of interrelation, we have carried out parallel measurements using much thicker dry films. As an example, we show in Figure 5 the plots of ψ and Δ for a 6000 Å dry film annealed at 50 °C against λ. In this case, both ψ and Δ show a completely different shape from that seen in Figure 3 for the thin film of 610 Å, and the progressive changes between consecutive ψ and Δ are more pronounced. The regular occurrences of peaks allow the progression of the scans with time to be followed more easily. To indicate the major expansion at the beginning of film immersion, the equivalent ψ and Δ profiles at $t = 0$ were also shown in Figure 5 (dashed lines), and the large gaps between the calculated pair of ψ and Δ and the first pair of the measured profiles again indicate the substantial expansion of the polymer fragments within the first minute of immersion. As before, these measured profiles were fitted using single uniform layer model, and the continuous lines shown in Figure 5 are the best fits at different time

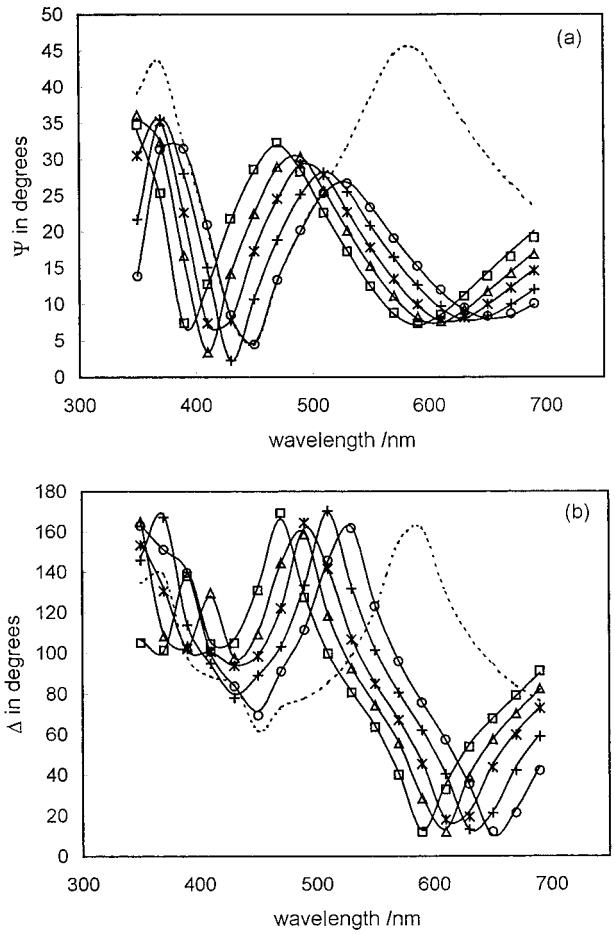

Figure 5. Variation of ψ (a) and Δ (b) with time for the swelling of a thin PC 100B film with a dry film thickness of 6000 ± 50 Å and annealed at 50 °C. The continuous lines are the best fits with structural parameters shown in Figure 5. The dotted lines were calculated assuming the film was immersed without any swelling or water penetration. The symbols represent the measurements at 1 (□), 3 (△), 6 (*), 16 (+), and 26 min (○) after water immersion.

intervals. The resultant plots of τ, n, and f_w vs $t^{0.5}$ are shown in Figure 6. Similar measurements for a 7200 Å dry film annealed at 150 °C are also shown in Figure 6 for comparison. The main observations obtained from Figure 6 are similar to those recorded from the swelling of thin films in that the films annealed at 50 °C swell much faster than those annealed at 150 °C and that the extent of water uptake for films annealed at the low temperature are twice as much as for those annealed at the high temperature.

The comparison of f_w obtained from changes in τ and n for the thick films is given in Figure 6c where it can be seen that the agreement is better than observed for the thin films, showing that as the dry film becomes thicker, the interrelation between τ and n is less serious. This result also indicates the linear increase of film thickness with water uptake and thus the proportional scaling of the total volume with that of the glassy polymer in the dry film. This consistency has been reported at the macroscopic scale with polymer samples of millimeter length scale.[38] But because our measurements were obtained for films below 1 μm, the linear relationship rules out the possibility of case II behavior that is often observed in many thick polymer films. The main feature of case II swelling is the presence of a penetrant concentration gradient across the film, char-

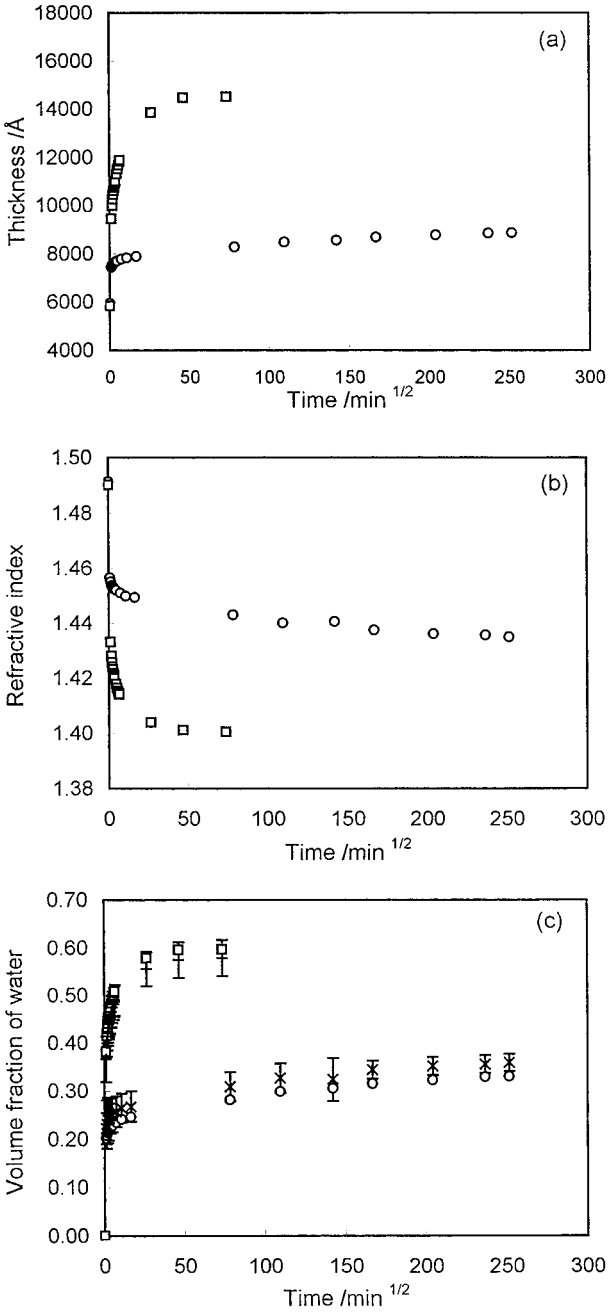

Figure 6. Change of thickness (a), refractive index (b), and water volume fraction (c) with time for the thin PC 100B films annealed at 50 (□) and 150 °C (○). Also in (c), the water volume fraction calculated from the change of thickness during film swelling is shown as (+) from the film annealed at 50 °C and as (×) from the film annealed at 150 °C.

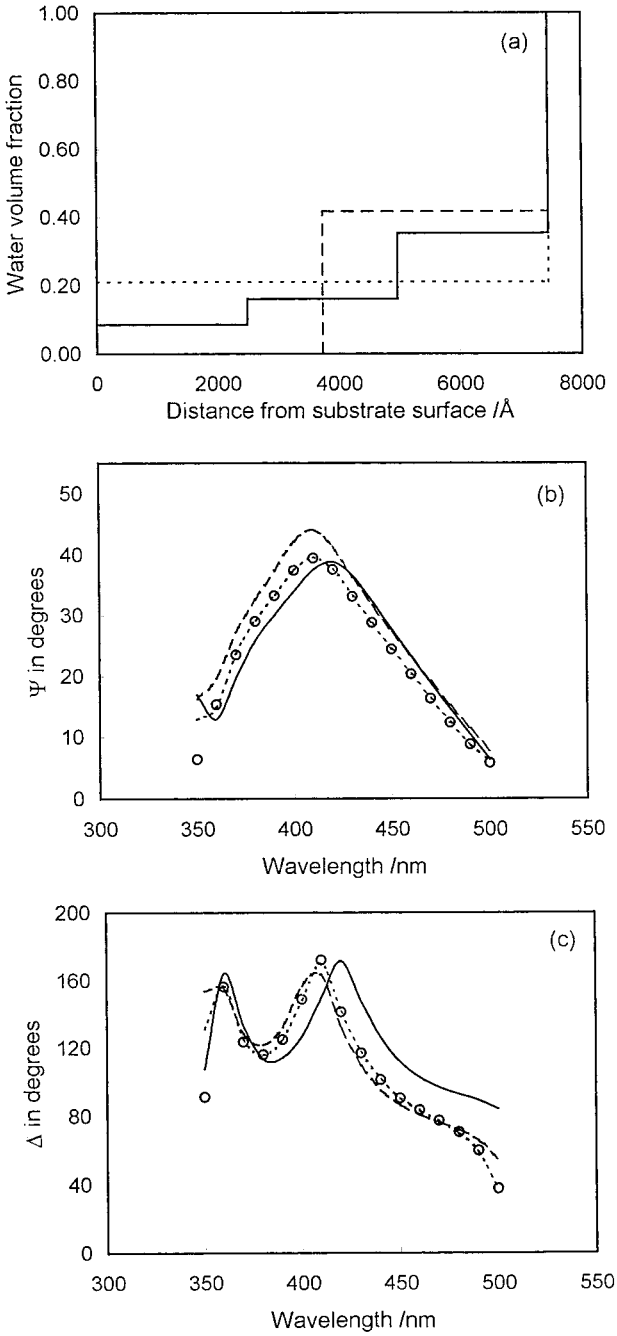

Figure 7. Volume fraction distributions (a) and the corresponding ψ (b) and Δ (c) calculated. The measured ψ (b) and Δ (c) are shown as (○), and the short dashed lines were calculated using the uniform layer model shown in (a) with a total thickness of 7450 ± 50 Å. As shown in (a), the first hyperthetical model assumes all the water is distributed within the outer half of the film, and the second model assumes a three-step profile with the volume fraction of water decreasing by a third as the inner part of the film is approached. The total amount of water is kept the same in each case.

acterized by a high water concentration on the outside of the film and a low water concentration in the inner part of the film.

It is customary and often convenient to analyze ellipsometric data using uniform layer model. In many cases this is because the data have no structural sensitivity to justify any more sophisticated models, and the uniform layer model is chosen due to its simplicity and the least number of parameters involved. Likewise, although the uniform layer model fits all the measured data well in this work, this itself does not warrant any uniqueness of the model. Other models representing nonuniform water distributions may also fit the data well. To verify this, we have assumed two idealized water density distributions mimicking the case II type of water sorption. The exact water density profiles are shown schematically in Figure 7a. Because nonuniform water distribution is most likely to occur in the course of swelling for the 6000 Å film annealed at 150 °C, the assessment has been set to test this situation. The water volume fraction obtained from the best uniform fit to the first pair of ψ and Δ under these conditions is also shown in Figure 7a for comparison (short dashed line). The total amount of water incorporated in the two

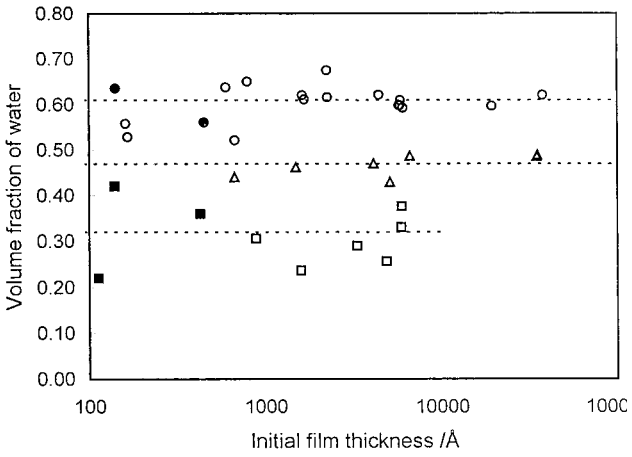

Figure 8. Water volume fraction in equilibrated PC100B films plotted against dry film thickness. Ellipsometry measurements made for films annealed at 50 °C are denoted as (○), for films annealed at 100 °C as (△), and for films annealed at 150 °C as (□). Neutron reflection measurements are shown as filled symbols with (●) for films annealed at 50 °C and (■) for films annealed at 150 °C.

nonuniform model distributions was assumed to be the same as that derived from the uniform layer model. The first nonuniform model assumes that the water only enters into the outer half of the film (long dashed line), and the thickness for this part of the polymer film goes up proportionally with the level of water uptake. The second nonuniform model assumes that the water distribution is divided into three equal steps, with the inner part being dry and the extent of water in the outer part being twice as much as that in the middle part of the layer (solid line). The calculated ψ and Δ profiles using these two nonuniform models are shown in Figure 7b,c together with the experimentally determined profiles. It can be seen from Figure 7 that neither of the two nonuniform models fits the measured ψ and Δ profiles. The uniform layer model is in fact the best representation to the water distribution within the film.

Figure 8 shows the variation of equilibrated water fraction in the swollen films ($f_{w,\infty}$) vs dry film thickness at all three annealing temperatures. To better display the variation over the thin thickness end, $f_{w,\infty}$ was plotted against log τ_0. To validate the $f_{w,\infty}$ values obtained from ellipsometric measurements, we have recently performed neutron reflection studies using the same PC polymer at the solid/water interface, and the resultant neutron data are also shown in Figure 8. We have purposely chosen to perform neutron measurements for dry films with $\tau_0 < 1000$ Å. As already indicated previously, over this thickness range it is difficult to decouple film thickness from water content using ellipsometric measurement, but neutron reflection is highly effective at separating the two parameters. The high sensitivity of neutron reflection arises partly from the much shorter neutron wavelength which makes it inherently more sensitive to the size at the angstrom level and partly from the use of D_2O to create a sharp isotopic contrast between water and PC polymer film. To justify the reliability of ellipsometric data over the large thickness range, the swelling of thick PC polymer films has also been examined by the gravimetric method. The thicknesses of the dry films used in the gravimetric analysis were mainly around 0.3 mm (not shown in Figure 8).

The dashed lines drawn through each set of data in Figure 8 are for guiding the eye only. Given that less number of neutron data points were obtained and the neutron data are scattered as much as the ellipsometric data, it is difficult to suggest any better quality of neutron results. However, because neutron reflection is intrinsically sensitive to the structural dimension at the order of hundreds of angstroms, the extent of scatter of neutron data is believed to be outside the resolution of the technique. Thus, the scatter of the data can only be attributed to the poor reproducibility intrinsic to the sample preparation. By averaging all the data from the two techniques, we can conclude that the mean values of $f_{w,\infty}$ are about 60% for the films annealed at 50 °C, 47% for those annealed at 100 °C, and 32% for those annealed at 150 °C. The data are within ±7% consistent with the values from the gravimetric method. These results thus show that the degree of film swelling and the subsequent water uptake are sensitive to the annealing temperature but are insensitive at all to the thickness of dry films. The latter statement is only valid at this level of data resolution. It might be expected that when films are below 1000 Å, the interactions between the surfaces and the film may affect the physical properties of the film,[39,40] thus forcing its swelling to deviate from the main trend observed for the thicker ones. The main interactions between PC polymer and the solid substrate are the affinity between the hydrophilic groups (PC and 2-hydroxypropyl) and silicon oxide and the silyl cross-linking between the trimethoxysilane groups and the hydroxyl groups on silicon oxide. As the thickness of the polymer film is reduced, the influence of these interactions may become more significant. The absence of any systematic deviation over the thin film range (see Figure 8) suggests that any surface related effects are either too weak to be detected or comparable to the range of errors.

The reduced film expansion with increasing annealing temperature may result from a combined effect of the improved structural organization within the films together with the strengthened silyl cross-linking network. Although ellipsometry measurements offer no information inside the films, it can be assumed that as temperature rises the fluidity within the films improves, and the hydrophobic and hydrophilic components become better segregated to form lamellar or other types of interwoven structures. The close packing of the hydrophobic layers within the film may work as a barrier to inhibit water sorption. The effect of temperature increase on the silyl cross-linking can be understood from inorganic sol−gel films cast on silicon oxide substrate, as described below.

Keddie et al.[41] examined the effect of temperature on the densification of SiO_2 sol−gel films using ion beam analysis and found that when the films were heated to 150 °C the film density was increased by some 10%. Accompanying this density increase is the decrease of hydrogen content within the films by a similar amount. These results indicate that with the increase of annealing temperature the number of siloxane groups (Si−O−Si) increases and that of silanol groups (Si−OH) decreases. The consolidation of the siloxane network with annealing temperature is entirely consistent with the trend of reduced swelling observed in PC 100B films. The only difference is the chemistry of cross-linking. In the case of sol−gel, the dehydration occurs between silanol groups, while in PC 100B the cross-linking occurs

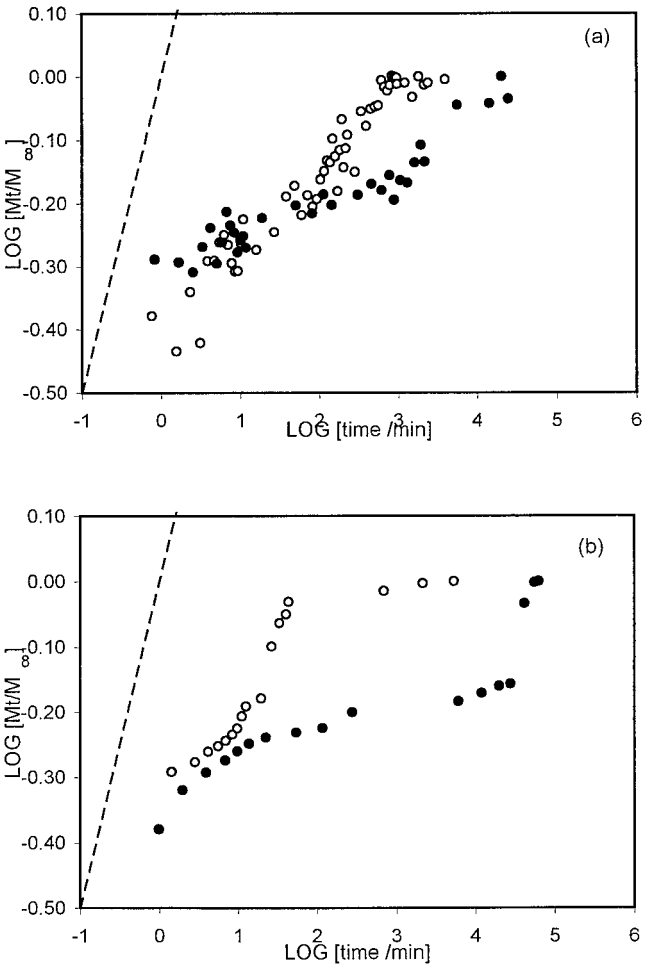

Figure 9. Plots of log[M_t/M_∞] vs log[time/min] to show the deviation of the rates of swelling from that of ideal Fickian process shown as dashed lines with a slope of 0.5. Films with dry thickness around 600 (a) and 6000 Å (b) were annealed at either 50 (○) or 150 °C (●).

both between methoxysilane groups and hydroxyl groups (including inorganic hydroxy groups on the surface of the substrate and organic hydroxy groups from 2-hydroxypropyl groups) and between methoxysilane groups themselves.

The variation of water volume fraction with time is clearly seen in Figures 4c and 6c. An alternative and yet more obvious way of showing the dynamic process of water sorption is to replot these data in terms of log-[M_t/M_∞] against log[time]. These profiles are shown in Figure 9a for the dry films of some 600 Å and in Figure 9b for those around 6000 Å. Note that the large differences in the shape of these plots from those shown in Figures 4 and 6 arise partly from the use of logarithmic plotting in Figure 9 and partly from the relationship between M_t/M_∞ and $(\tau - \tau_0)/(\tau - \tau_\infty)$ as given in eq 2. This type of data plotting allows a more obvious assessment of the dependence of dynamic swelling on annealing temperature. In these plots the effect of annealing temperature on film swelling is largely reflected in the change of slopes of the profiles. For example, Figure 9a shows that for thin films annealing at the lower temperature of 50 °C gives a greater slope and hence a faster swelling. This trend is seen for films with greater dry thicknesses, though in a more complex way as will be explained below. However, these results altogether indicate a relatively minor dependence of the swelling process on dry film thickness.

Each swelling profile shown in Figure 9 can be approximately treated as a swelling process consisting of two main steps. The first step occurs within the first minute of film immersion in water and involves the transport of some 50% water into the film. Because this process is fast, it is not unreasonable to assume that the swelling over this period is controlled by Fickian diffusion. Because the simple characteristics of Fickian diffusion is the linear proportion of M_t/M_∞ to $t^{0.5}$, the two dashed lines shown in Figure 9 were drawn with a slope of 0.5. The intercepts of the two dashed lines were arbitrarily set to go through the axial origins. The transformation of the swelling from the simple diffusion-controlled process to an increasingly relaxation-controlled one is reflected on the further deviation of the slopes from that indicated by the dashed line. It is clear that, over the first half of the second step, increase in annealing temperature slows down swelling, as evident from the change of the average slopes. The second half of the second step is characterized by the uprising of the profiles and hence increased slopes. This is clearly seen from Figure 9b for the thick films, though less evident for thin films shown in Figure 9a. Such increased swelling is likely to be caused by the rehydration of C−O−Si bonds formed between organic hydroxy groups and methoxysilanes during annealing. C−O−Si bonding is relatively labile and is expected to be the main type of cross-linking in the bulk of the film because of its dominant molar fraction in the polymer. The difference in the onset of this accelerated swelling stage implies the attachment of a certain fraction of C−O−Si bonds below which rehydration alters the rate of structural relaxation. Furthermore, the results shown in Figure 9 show that, for films with similar dry film thicknesses, the rates of the swelling during this final part are comparable. It can also be seen from Figure 9 that under a given annealing temperature thicker films tend to swell faster, indicating less structural constraints within them.

Conclusion

The swelling of PC 100B films consists of two distinct steps. The initial fast swelling is controlled by the classical Fickian diffusion, and the subsequent slow swelling process is controlled by polymer fragment relaxation. Each step approximately contributes to about 50% of the total water uptake. Change in annealing temperature has little effect on the fast initial swelling but does have a significant effect on the dynamic relaxation of polymer fragments. While films annealed at 50 °C reaches equilibration in less than 1 day, it takes some 30 days for those annealed at 150 °C to approach their full swollen state. The faster swelling must have resulted from the faster relaxation and more imperfect siloxane structuring. The observed trend of swelling is also consistent with the possible formation of aggregated structures within the films although ellipsometry has no sensitivity in detecting such mesoscopic morphology.

Apart from its effect on the kinetic process of swelling, annealing temperature was also found to have a profound effect on the equilibrated water volume fraction in the film. The final water uptake of the film is determined by its expandability that is in turn governed by the extent of silyl reaction. Hence, annealing temperature is a very effective handle in controlling the dynamic, mechanical, and physical properties of PC 100B films.

Although the two-stage swelling processes have been reported some 30 years for homogeneous polymer matrices such as PMMA and PS under certain combinations of film thicknesses and solvent conditions, there is still no reliable theoretical model that can predict the relative contributions of the two simultaneous processes. Hopfenberg et al.[7−9] have developed an analytical formula that assumes the simple addition between the Fickian diffusion and relaxation process. But because there is no clear physicochemical significance to the relaxation terms, the application of this equation has largely been a curve-fitting exercise. This, together with the fact that our polymer has a distinctly heterogeneous structural feature, suggests that future effort needs to be made to develop a more theoretically sound model to help interpret the molecular events occurred during the swelling of these hydrogel films.

References and Notes

(1) Thomas, N. L.; Windle, A. H. *Polymer* **1978**, *19*, 255.
(2) Thomas, N. L.; Windle, A. H. *Polymer* **1980**, *21*, 613.
(3) Thomas, N. L.; Windle, A. H. *Polymer* **1982**, *23*, 529.
(4) Hopfenberg, H. B.; Nicolais, L.; Drioli, E. *Polymer* **1976**, *17*, 195.
(5) Alfrey, A.; Gurnee, E. F.; Lloyd, W. G. *J. Polym. Sci.* **1966**, *C12*, 249.
(6) Hopfenberg, H. B.; Holley, H. M.; Stannet, V. *J. Polym. Eng. Sci.* **1969**, *9*, 249.
(7) Berens, A. R.; Hopfenberg, H. B. *Polymer* **1978**, *19*, 489.
(8) Enscore, D. J.; Hopfenberg, H. B.; Stannett, V. T. *Polymer* **1977**, *18*, 793.
(9) Crank, J. *The Mathematics of Diffusion*, 2nd ed.; Clarendon Press: Oxford, 1975.
(10) Peppas, N. A.; Khare, A. R. *Adv. Drug Delivery Rev.* **1993**, *11*, 1.
(11) Colombo, P. *Adv. Drug Delivery Rev.* **1993**, *11*, 37.
(12) Crank, J., Park, G. S., Eds.; *Diffusion in Polymers*; Academic Press: New York, 1968.
(13) Sutandar, P.; Dong, J. A.; Elias, I. F. *Macromolecules* **1994**, *27*, 7316.
(14) Ercken, M.; Adriaensens, P.; Reggers, G.; Carleer, R.; Vanderzande, D.; Gelan, J. *Macromolecules* **1996**, *29*, 5671.
(15) McDonald, P. J. *Prog. Nucl. Magn. Res. Spectrosc.* **1997**, *30*, 69.
(16) Lane, D. M.; McDonald, P. J. *Polymer* **1997**, *38*, 2329.
(17) Goerke, U.; Chamberlain, A. H. L.; Crilly, E. A.; McDonald, P. J. *Phys. Rev. E: Part B* **2000**, *62*, 5353.
(18) Drake, P. A.; Bohn, P. W. *Appl. Spectrosc.* **1996**, *50*, 1023.
(19) Drake, P. A.; Bohn, P. W. *Anal. Chem.* **1995**, *67*, 1766.
(20) Hassan, M. M.; Durning, C. J. *J. Polym. Sci.* **1999**, *37*, 3159.
(21) Durning, C. J.; Hassan, M. M.; Tong, H. M.; Lee, K. W. *Macromolecules* **1995**, *28*, 4234.
(22) Wu, W. L.; Orts, W. J.; Majkrzak, C. J.; Hunston, D. L. *Polym. Eng. Sci.* **1995**, *35*, 1000.
(23) Lin, H.; Steyerl, A.; Satija, S. K.; Karim, A.; Russell, T. P. *Macromolecules* **1995**, *28*, 1470.
(24) Yim, H.; Kent, M.; McNamara, W. F.; Ivkov, R.; Satija, S.; Majewski, J. *Macromolecules* **1999**, *32*, 7932.
(25) Filippova, N. L. *J. Colloid Interface Sci.* **1999**, *212*, 589.
(26) Styrkas, D.; Doran, S. J.; Gilchrist, V.; Keddie, J. L.; Lu, J. R.; Murphy, E.; Sackin, R.; Su, T. J.; Tzizinou, A. In *Polymer Surfaces and Intefaces III*; Richards, R. W., Peace, S. K., Eds.; Wiley: Chichester, 1999; p 1.
(27) Chen, W. L.; Shull, K. R.; Papatheodorou, T.; Styrkas, D. A.; Keddie, J. L. *Macromolecules* **1999**, *32*, 136.
(28) Tiberg, F.; Brinck, J.; Grant, L. *Curr. Opin. Colloid Interface Sci.* **1999**, *4*, 411.
(29) Murphy, E. F.; Lu, J. R.; Brewer, J.; Russell, J.; Penfold, J. *Langmuir* **1999**, *15*, 1313.
(30) Murphy, E. F.; Lu, J. R.; Lewis, A. L.; Brewer, J.; Russell, J.; Stratford, P. *Macromolecules* **2000**, *33*, 4545.
(31) Murphy, E. F.; Keddie, J.; Lu, J. R.; Brewer, J.; Russell, J. *Biomaterials* **1999**, *20*, 1501.
(32) Lewis, A. L.; Hughes P. D.; Kirkwood, L. C.; Leppard, S. W.; Redman, R. P.; Tolhurst, L. A.; Stratford, P. W. *Biomaterials* **2000**, *21*, 1847.
(33) Lewis, A. L.; Cumming, Z. C.; Goreish, H. H.; Kirkwood, L. C.; Tolhurst, L. A.; Stratford, P. W. *Biomaterials* **2001**, *22*, 99.
(34) J.A. Woollam Company. *The Users Manual of Variable Angle Spectroscopic Ellipsometry*; J.A. Woollam Company: Lincoln, NE, 1992.
(35) Azzam, R. M. A.; Bashara, N. M. *Ellipsometry and Polarized Light*; North-Holland: Amsterdam, 1977.
(36) Born, M.; Wolf, E. *Principles of Optics*; University Press: Cambridge, 1997.
(37) Guo, S.; Gustafsson, G.; Hagel, O. J.; Arwin, H. *Appl. Opt.* **1996**, *35*, 1693.
(38) Peppas, N. A. *Hydrogels in Medicine and Pharmacy;* CRC: Boca Raton, FL, 1987; Vol. 1.
(39) Zheng, X.; Rafailovich, M. H.; Sokolov, J.; Strahemechny, Y.; Schwarz, S. A. *Phys. Rev. Lett.* **1997**, *79*, 241.
(40) Keddie, J. L.; Jones, R. A. L.; Cory, R. A. *Faraday Discuss.* **1994**, *98*, 219.
(41) Keddie, J. L.; Giannelis, E. P. *J. Am. Ceram. Soc.* **1990**, *73*, 3106.

MA010476I